Macromolecules
ARTICLE

Macromolecules **2010**, *43*, 1507–1514 **1507**
DOI: 10.1021/ma9021604

Self-Assembly and Hierarchies in Pyridine-Containing Homopolymers and Block Copolymers with Hydrogen-Bonded Cholesteric Side-Chains

Juuso T. Korhonen,[†] Tuukka Verho,[†] Patrice Rannou,*[,‡] and Olli Ikkala*[,†,‡]

[†]*Department of Applied Physics, Helsinki University of Technology, P.O.Box 5100, FIN-02015 TKK, Espoo, Finland and* [‡]*Laboratoire d'Electronique Moléculaire, Organique et Hybride, UMR5819-SPrAM (CEA/CNRS/Université J. FOURIER-Grenoble I), INAC, CEA-Grenoble, 17 Rue des Martyrs, F-38054 Grenoble Cedex 9, France*

Received September 29, 2009; Revised Manuscript Received December 23, 2009

ABSTRACT: We investigate supramolecular complexes where a mesogenic molecule, cholesteryl hemisuccinate (CholHS), is hydrogen-bonded to a homopolymer, poly(4-vinylpyridine) (P4VP), to allow liquid crystallinity and to block copolymer polystyrene-*block*-poly(4-vinylpyridine) (PS-*b*-P4VP), to allow hierarchical self-assembly. Blends of P4VP and CholHS (with one or less CholHS molecules vs each pyridine group) form microphase separated smectic A (SmA) structures where the periods correspond to a head-to-head arrangement of the mesogens, based on small angle X-ray scattering (SAXS), polarized optical microscopy (POM), as supported by differential scanning calorimetry (DSC). Heating leads to an isotropic melt. Liquid crystallinity is most stable at low degrees of CholHS complexation, whereas at high degrees of complexation competing effects due to CholHS crystallization may take place, depending on the thermal history. When CholHS is complexed with PS-*b*-P4VP, hierarchical structure-*within*-structure morphologies are observed, based on SAXS but also directly visualized using transmission electron microscopy (TEM). The inner structure is smectic and the larger structure depends on the volume fractions of the corresponding blocks. The morphologies are mapped for different complexation ratios and different molecular weights. The shown hierarchies can be useful to construct functional self-assemblies.

Introduction

Self-assemblies and their hierarchies have extensively been used to control material properties at different length scales.[1−10] One general approach is based on polymers where side groups are connected in a supramolecular manner using ionic interactions, coordinations, or hydrogen bonds, where the most straightforward supramolecular side groups are plain amphiphiles or surfactants, which allow control of self-assembly, polymer backbone stretching, and even conductivity.[3,11−19] In the case of polypeptides, they also allow control of the secondary structures in addition to self-assembly.[20−24] More functional side-chains comprise mesogenic groups that allow supramolecular side-chain liquid crystalline polymers upon complexing with homopolymers and block copolymers.[25−28] The side chains can also be photoisomerizable, which leads to optically controllable materials.[29−31]

Cholesterol is the first mesogenic moiety investigated.[32] Cholesteryl-containing compounds are common in biological materials and in synthetic materials its shape persistence in combination with chirality has encouraged to combine it in a large number of systems.[33−42]

Previously it has been shown that pentadecylphenol is a particularly useful supramolecular additive, which allows self-assemblies by hydrogen bonding to pyridine containing polymers, such as poly(4-vinylpyridine) (P4VP).[13,18,43,44] Here we investigate cholesteryl hemisuccinate (CholHS) and show that it hydrogen bonds to P4VP in many respects the same way as pentadecylphenol. This is interesting, because the pyridine−carboxylic acid hydrogen bonding, probably in combination with the ethyl spacer of CholHS, dominates the dimerization between two CholHS molecules. Also, learning the ways to prepare supramolecular complexes based on cholesteryl−containing materials could be of interest in the context of induced chirality (of the wide literature, see, e.g., ref 45). We point out that previously there has been interesting work on complexation of CholHS to poly(dimethylamino ethyl methacrylate) where ionic interaction has been used for the bonding.[35] This contrasts the typically weaker and more dynamic hydrogen bonds used in this work.

Here we first investigate interactions between P4VP and CholHS using two molecular weights of P4VP, and investigate the liquid crystallinity using polarized optical microscopy, transmission electron microscopy, and small-angle X-ray scattering. Finally formation of hierarchical structures in polystyrene-*block*-poly(4-vinylpyridine) complexes with CholHS are studied.

Experimental Section

Materials. High molecular weight P4VP was obtained from Polysciences, Inc. and all other polymers and copolymers from Polymer Source, Inc. The polymers were used without further purification. Specifications of the polymers are gathered in Table 1. Cholesteryl hemisuccinate was acquired from Sigma-Aldrich. All materials were dried at 60 °C in a vacuum oven for in excess of 12 h prior to use. Analytical grade chloroform was obtained from Sigma-Aldrich and used as received. Schematic representations of the molecules are shown in Figure 1.

Sample Preparation. The dried compounds were dissolved in chloroform separately at low concentrations of 2% (w/w) in order to ensure homogeneous mixtures and then stirred for 12 h or more before they were mixed in the desired ratios. Complexes with nominal ratio of CholHS molecules versus 4-vinylpyridine

*Corresponding authors. E-mail: (O.I.) olli.ikkala@tkk.fi; (P.R.) patrice.rannou@cea.fr.

Published on Web 01/15/2010

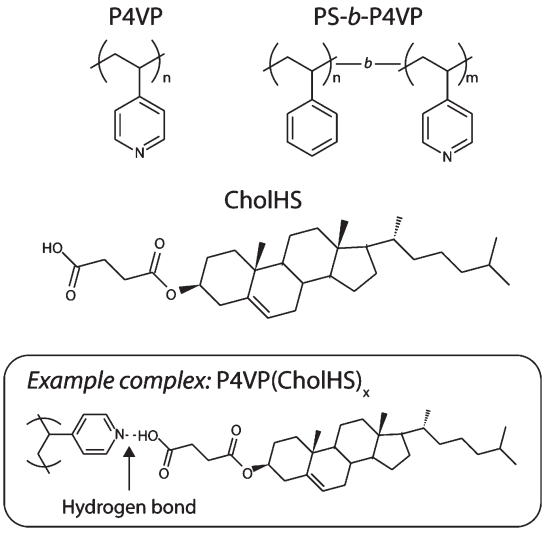

Figure 1. Homopolymer P4VP, block copolymer PS-*b*-P4VP, and the mesogenic amphiphile CholHS. An example of a nominally fully complexed case is shown.

Table 1. The Polymers Used

	P4VP M_w (g/mol)	PS M_w (g/mol)	M_w/M_n
$P4VP_{5.4k}$	5400		1.06
$P4VP_{50k}$	50 000		
PS_{40k}-*b*-$P4VP_{5.6k}$	5600	40 000	1.09
PS_{252k}-*b*-$P4VP_{43k}$	43 000	252 000	1.09
PS_{422k}-*b*-$P4VP_{63k}$	63 000	422 000	1.09

repeat units (i.e., nominal degree of complexation) of 0.25, 0.50, 0.75, and 1.00 were prepared for $P4VP_{5.4k}$, $P4VP_{50k}$, and PS_{40k}−$P4VP_{5.6k}$. For other polymers, only nominally fully complexed samples were prepared. Pure polymers and neat CholHS were also characterized. The resulting mixtures were stirred additionally for at least 2 days after which they were evaporated slowly under ambient conditions to achieve the bulk samples.

Fourier-Transform Infrared Spectroscopy. Fourier-transform infrared spectra (FT-IR) were recorded on a Nicolet 380 FT-IR spectrometer in transmission mode. A drop of chloroform solution was evaporated on a newly pressed dry potassium bromide pellet and averaging over 64 scans was used to record spectra with 2 cm^{-1} resolution at room temperature.

Differential Scanning Calorimetry. Thermal transitions in samples were investigated using a Mettler-Toledo Star^e differential scanning calorimeter (DSC). Heating rate used was 10 °C/min and the measurement consisted of three cycles of heating to 210 °C and cooling to −20 °C. The glass transition temperatures were estimated from the second heating cycle by taking the midpoint of the transition step. To locate the isotropic transition temperatures, Gaussian type functions were fitted to the transition peaks for both heating and cooling curves of the second cycle.

Small-Angle X-ray Scattering. The instrument consists of a Bruker Microstar microfocus X-ray source with a rotating anode emitting CuK_α radiation (λ = 1.54 Å), Montel optics, and four sets of collimating JJ X-ray four-blade slits, resulting in about 1 mm × 1 mm beam area at the sample. Bruker AXS 2-D detector was placed at a 0.59 m distance from sample. The magnitude of scattering vector is given by $q = (4\pi/\lambda) \sin \theta$, where 2θ is the scattering angle. Bulk samples were annealed at 200 °C for 15 min and cooled back to room temperature before SAXS measurements. Two samples, namely $P4VP_{5.4k}(CholHS)_{0.25}$ and $P4VP_{5.4k}(CholHS)_{0.50}$, were investigated in detail in heating and cooling to assess the reversibility of the transitions and the samples were not subjected to heat treatment prior to measurements. These samples were enclosed between a Mylar film and Kapton tape and the samples were placed on a Linkam HFS 91 sample heating stage with a Linkam TP 93 temperature controller. A constant nitrogen flow through the sample chamber was kept during the measurements. For $P4VP_{5.4k}(CholHS)_{0.25}$ the scattering patterns were recorded from 40 to 160 °C and back to 40 °C at 10−20 °C intervals using 5 min data collection time. In case of $P4VP_{5.4k}(CholHS)_{0.50}$ an additional heating/cooling cycle from 40 to 220 °C and back was made after the first cycle. Other compositions were screened with a simpler arrangement: they were enclosed between two Mylar films and they were collectively heated to the desired temperature after which scattering data was collected for 30 min per sample. Scattering patterns were collected at 40, 80, 120, and 160 °C in that order.

Transmission Electron Microscopy. Bright-field transmission electron microscope (TEM) images were recorded on a FEI Tecnai 12 TEM operating at an acceleration voltage of 120 kV. Here, 40−70 nm thick sections were sliced at −60 °C with a Leica Ultracut UCT ultramicrotome using a cryo 25° Diatome diamond knife. Slices were collected on lacey carbon support film grids. Samples were then stained at room temperature either in iodine or in ruthenium tetroxide vapors for ca. 30 min in order to improve the contrast. Longer staining times were used for block copolymer samples (typically 2 h for iodine).

Polarized Optical Microscopy. Birefringence in samples was observed using a Leica DM4500P optical microscope (POM) equipped with crossed polarizers. Images were taken using a Leica DFC 420 camera. A drop of sample was cast from chloroform onto a microscope slide and covered with a cover slide. The samples were then individually placed on a Linkam HFS 93 or LTS 350 heating stage controlled either by a Linkam TP 93 or TMS 94 temperature controller. A constant nitrogen flow through the heating stage was upheld to hinder chemical decomposition. Several heating/cooling cycles with varying heating rates were monitored. To investigate the liquid crystalline textures, the samples were first heated to the isotropic state and then the birefringent textures were observed at different temperatures using several cooling rates. Such observations also gave indirect information on the hydrogen bonding stability of the complexes at elevated temperatures.

Results and Discussion

Complex Formation. Interaction between the carboxylic acid group of CholHS and the 4-vinylpyridine nitrogens of P4VP was first investigated using FT-IR. Figure 2 shows the 1600 cm^{-1} region of the FT-IR spectra for $P4VP_{5.4k}(CholHS)_x$ and $P4VP_{50k}(CholHS)_x$. P4VP has a distinct absorption peak at 1597 cm^{-1}, corresponding to a resonant absorption mode of the pyridine ring.[13,46] This peak is known to shift to higher wavenumbers due to interactions, e.g. large shift to ca. 1640 cm^{-1} due to protonation by strong acids, smaller shift to ca. 1620 cm^{-1} due to metal coordination, and relatively small shift to ca. 1604 cm^{-1} due to phenolic hydrogen bonding.[13,47,48] Figure 2 shows a small but clear shift to 1607 cm^{-1} upon mixing CholHS and P4VP, which suggests hydrogen bonding. CholHS has no distinct absorption peaks in this region, which suggests that the peak is the same resonant peak as in the neat pyridine but shifted. The areas under the peaks and the peak positions were estimated by fitting pseudo-Voigt-type functions to the data. The intensity of the shifted peak at 1607 cm^{-1} vs the original peak at 1597 cm^{-1} increases as the nominal degree of complexation is increased. The fraction of hydrogen-bonded 4-vinylpyridines can be estimated using refs 49 and 50

$$f_{HB}^{N} = \frac{A_{1607}}{A_{1607} + \frac{\alpha_{1597}}{\alpha_{1607}} A_{1597}}$$

where A and α are the peak areas and absorption coefficients at 1607 and 1597 cm^{-1}. By studying a blend of poly(2-vinylpyridine) and a carboxylic acid polymer and using a

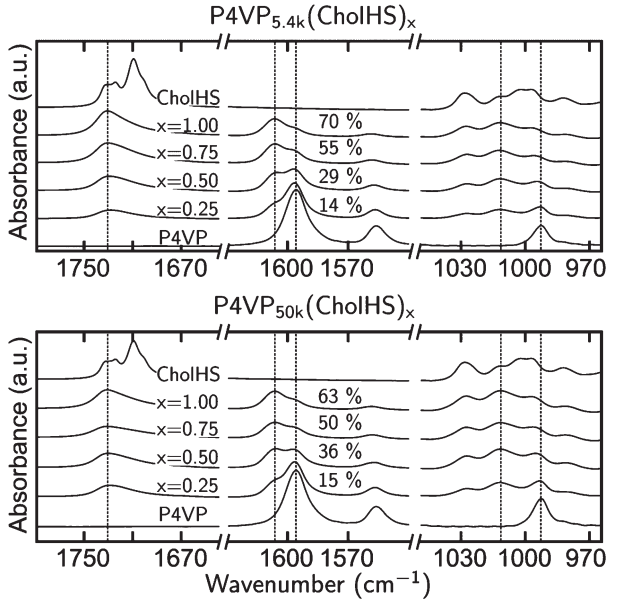

Figure 2. Interaction of P4VP and CholHS investigated by FT-IR using two molecular weights of P4VP. The absorption band of P4VP at 1597 cm^{-1} is shifted to 1607 cm^{-1} due to hydrogen bonding of CholHS to the pyridines. The percentage denotes the area of the 1607 cm^{-1} peak compared to the sum of the complexed (1607 cm^{-1}) and uncomplexed (1597 cm^{-1}) peaks, indicating that the true degree of complexation is lower than the nominal ratio, as the absorption cross sections do not change significantly in complexation. P4VP has an absorption band at 993 cm^{-1}, which is shifted to around 1011 cm^{-1}. A hydrogen bond free carboxyl stretching mode at 1733 cm^{-1} is observed in P4VP−CholHS complexes, whereas in pure CholHS a major downshift is observed, indicating dimerization.

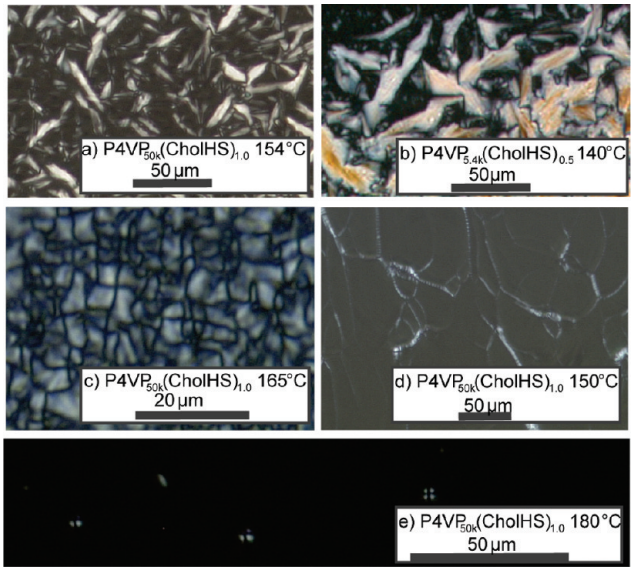

Figure 3. Polarized optical micrographs supporting SmA liquid crystallinity: (a) $P4VP_{50k}(CholHS)_{1.0}$ at 154 °C during cooling from isotropic state showing bâtonnets; (b) $P4VP_{5.4k}(CholHS)_{0.5}$ at 140 °C during cooling from isotropic state also showing bâtonnets, but now for lower x and the smaller molecular weight of P4VP; (c) $P4VP_{50k}(CholHS)_{1.0}$ at 165 °C showing fan-shaped textures; (d) $P4VP_{50k}(CholHS)_{1.0}$ at 150 °C showing oily streaks; (e) $P4VP_{50k}(CholHS)_{1.0}$ at 180 °C showing a homeotropically aligned SmA mesophase with a few SmA defects.

reference absorption peak that is unaffected by the hydrogen bonding, Lee et al. showed[49] that the absorption cross sections for pyridine did not change upon hydrogen bonding. Similarly, using an inert FT-IR absorption at 1557 cm^{-1} as a reference, we confirmed here that a similar reasoning is valid also in the present case. Therefore, the absorption cross sections of the free and hydrogen-bonded P4VP bands at 1597 and 1607 cm^{-1} do not change significantly upon complexation, i.e. $\alpha_{1597}/\alpha_{1607} \approx 1$. Now, the actual degree of complexation can be estimated to be 60−70% of the nominal degree of complexation (see Figure 2) with only a slight saturation at high values of x.

Figure 2 also displays the 1000 cm^{-1} region of the FT-IR spectra. P4VP has an absorption peak related to pyridine stretching at 993 cm^{-1},[13] whose intensity is observed to decrease upon complexation with CholHS. Near that band, CholHS has overlapping absorption peaks, which makes quantitative analysis difficult. Still, the reduced absorption at 993 cm^{-1} and increased absorption at 1011 cm^{-1} qualitatively further confirm that the pyridine groups take part in hydrogen bonding.

Finally, the carbonyl absorption bands are addressed.[50] In pristine CholHS, there are three absorption peaks at 1710, 1725, and 1733 cm^{-1} (see Figure 2). As will be shortly discussed, 1733 cm^{-1} is here assigned to free >C=O groups that do not undergo hydrogen bonding. The downshifted bands at 1710 and 1725 cm^{-1} are here assigned to hydrogen bonded dimerization between two CholHS molecules. However, in P4VP−CholHS complexes the absorption is observed only at 1733 cm^{-1}, suggesting that all >C=O groups are essentially free of hydrogen bonds. Importantly, this suggests that in P4VP/CholHS mixtures the 4-vinylpyridine−carboxylic acid hydrogen bonding dominates over the carboxylic acid dimerization. Related observations were made in another context between pyridine functionalized polyglycerol and CholHS.[37] Incidentally, the discussed FT-IR-shifts due to hydrogen bonding between P4VP and CholHS are quite similar to those observed between P4VP and alkylphenols, which are also shown lead to self-assemblies but without mesogenic moieties.[13]

Previously a model system of 4,4′-bipyridine and CholHS has been investigated,[38] and hydrogen bonding was demonstrated from FT-IR O−H···N bands at 2500 and 1920 cm^{-1}. These bands were reported to be stable up to 168 °C. Also we observe bands at 2490 and 1940 cm^{-1} in the complexes (see Supporting Information), but they are too weak for quantitative analysis. Anyhow these bands further confirm the existence of the hydrogen bonding.

Thermal Transitions. The $P4VP(CholHS)_x$ complexes show liquid crystallinity as will next be demonstrated using several techniques. First $P4VP_{50k}(CholHS)_{1.0}$ is discussed. The large degree of complexation promotes fluidity at elevated temperatures and leads to particularly clear liquid crystalline textures in polarized optical microscopy. Near room temperature the complex is glassy and birefringent, whereas heating past 194 °C leads to nonbirefringent isotropic fluid. Cooling leads to characteristic smectic A (SmA) liquid crystalline textures, as shown by several examples at different temperatures: Figure 3a gives an example of bâtonnets at 154 °C during the early development of LC texture. Figure 3c shows fan-like texture at 165 °C, Figure 3d shows oily streaks at 150 °C, and Figure 3e shows a homeotropically aligned SmA mesophase, appearing as a featureless black image for a SmA monodomain under POM imaging conditions (with a few homogeneously aligned SmA defects), which can be obtained upon pressing the microscope coverslip against the bottom glass plate at 180 °C. Qualitatively similar behavior was observed in POM for all of the complexes $P4VP(CholHS)_x$ with x = 0.25, 0.50, 0.75, 1.0 and both M_w, even if the level of

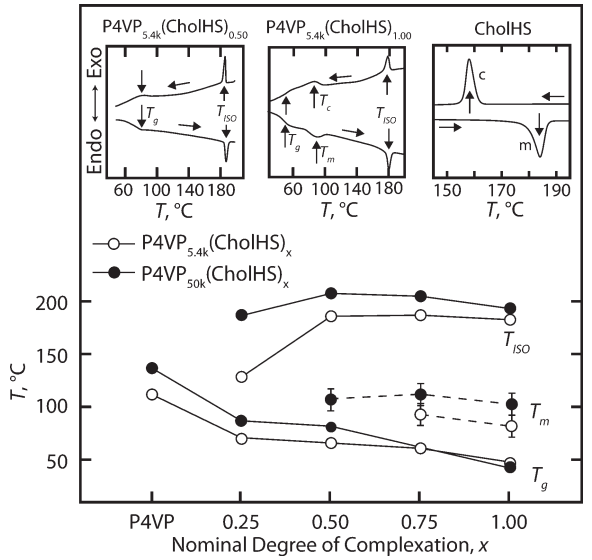

Figure 4. T_g, T_m, and T_{ISO} for P4VP(CholHS)$_x$ based on DSC second heating cycle. Insets show examples of DSC thermograms: In the left inset P4VP$_{5.6k}$(CholHS)$_{0.50}$ shows the glass transition and isotropization temperatures. In the center inset P4VP$_{5.6k}$(CholHS)$_{1.00}$ shows an additional transition, which we assign as the side-chain crystallization. In the right inset is shown the crystallization and melting of pure CholHS.

birefreingence in the first one is smaller. As an example, Figure 3b shows bâtonnets for the lower molecular weight complex with $x = 0.5$.

DSC was used to locate the thermal transitions, see Figure 4. The neat homopolymers P4VP$_{50k}$ and P4VP$_{5.4k}$ are amorphous and show glass transitions T_g at 138 °C (see Figure 4) and 113 °C, respectively. Therefore, T_g is reduced for small molecular weight of the polymer, as expected. The neat CholHS is crystalline with a melting point at ca. 186 °C and crystallization at ca. 160 °C using a sweep rate of 10 °C/min, thus showing a considerable hysteresis (see Figure 4 right inset). Figure 4 and middle inset illustrate that hydrogen bonding of CholHS to P4VP allows considerably reduced T_g due to plasticization by the spacer-like CholHS supramolecular side-chains in analogy with related materials where pentadecylphenol is hydrogen bonded to P4VP.[43,51] Endothermic peaks upon heating accompanied by exothermic peaks upon cooling were observed at high temperatures (see middle inset of Figure 4), which can be identified as T_{ISO} from self-assembled liquid crystalline state to the isotropic state, see later also SAXS data. T_{ISO} of P4VP$_{5.4k}$(CholHS)$_x$ and P4VP$_{50k}$(CholHS)$_x$ are relatively constant in the range 180−210 °C for $x \geq 0.5$, and it is strongly reduced for $x = 0.25$. Figure 4 also shows that T_{ISO} is slightly lower for the lower molecular weight P4VP. Note that middle inset illustrating the thermogram of P4VP(CholHS)$_{1.0}$ also shows an additional endotherm upon cooling and the corresponding exotherm in heating in the range 80−110 °C. We preliminarily interpret such a transition as side-chain crystallization of the CholHS molecules hydrogen bonded to the P4VP chains, to be discussed later.

Transmission Electron Microscopy. We next investigated whether the smectic layers could be resolved in TEM to give unambiguous interpretation on the lamellar self-assemblies. Figure 5 shows TEM images of P4VP$_{5.4k}$(CholHS)$_x$ with $x = 0.5$ and 1.0. Layered structure is observed in both cases in agreement with the proposed smectic liquid crystallinity and $x = 1.0$ suggests better long-range ordering than that of the $x = 0.5$ sample. Fourier-transform patterns suggest that

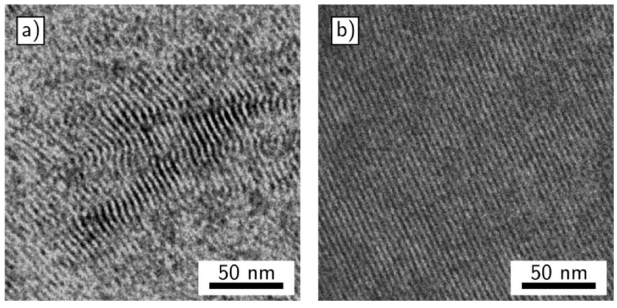

Figure 5. TEM images of RuO_4-stained (a) P4VP$_{5.4k}$(CholHS)$_{0.5}$ and (b) P4VP$_{5.4k}$(CholHS)$_{1.0}$ at room temperature, where the SmA layered structure is frozen to lead to solid material.

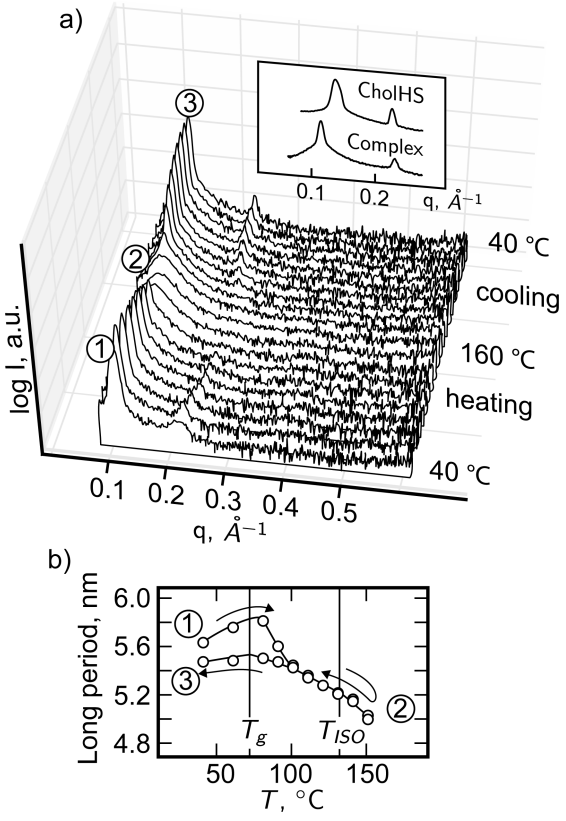

Figure 6. SAXS patterns upon heating and cooling for P4VP$_{5.4k}$(CholHS)$_{0.25}$. (a) Smectic order at room temperature, isotropization upon heating past 150 °C, and recovery of the smectic order upon cooling. (b) Periodicity of the smectic order in P4VP$_{5.4k}$(CholHS)$_{0.25}$, also indicating its stepwise reduction in the first heating upon passing T_g.

in both cases the periodicity is in the range of 4−5 nm. More quantitative estimates will be given later using SAXS. The samples were stained with either ruthenium tetroxide or iodine to increase contrast. Both agents increased contrast compared to the unstained samples, where only a very slight contrast between the possibly crystalline CholHS and amorphous polymer could be seen.

Small Angle X-ray Measurements. We will first discuss P4VP(CholHS)$_x$ with low nominal degree of complexation and lower molecular weight M_w = 5400 g/mol. Figure 6a depicts clear SAXS reflections for P4VP$_{5.4k}$(CholHS)$_{0.25}$ at the magnitude of the scattering vector $q = 0.112$ Å^{-1} and the second order reflection at a position corresponding to double angle at 0.227 Å^{-1} (see label "1" in Figure 6a), thus agreeing smectic structure with a period of ca. 5.6 nm. As such

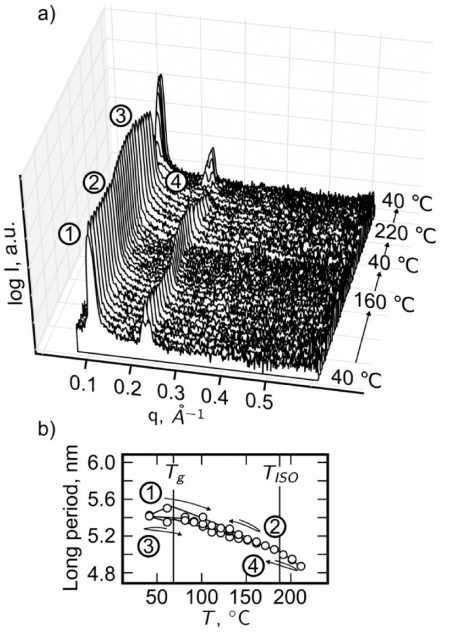

Figure 7. SAXS patterns upon heating and cooling for P4VP$_{5.4k}$-(CholHS)$_{0.50}$. (a) Reversibility illustrated by first heating to 160 °C, cooling down to room temperature, heating to 220 °C to show isotropization, and finally cooling down to show recovery of the smectic order. (b) Smectic periodicity as a function of temperature. In this case, the step upon passing T_g in the first heating is much smaller than in the case of $x = 0.25$ due to more efficient plasticization.

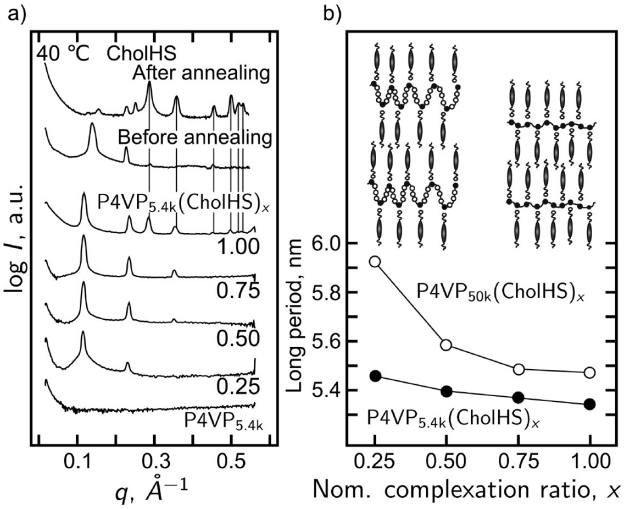

Figure 8. (a) SAXS reflection of P4VP(CholHS)$_x$ with the molecular weight $M_w = 5400$ g/mol at 40 °C as well as the SAXS reflection of the neat CholHS crystals before annealing and after annealing at 220 °C. (b) Smectic periodicities of P4VP(CholHS)$_x$ with $M_w = 5400$ g/mol and $M_w = 50\,000$ g/mol based on SAXS. The left inset illustrates larger periodicity for small x when only a fraction of P4VP repeat units are hydrogen bonded to CholHS molecules. The right inset shows a smaller periodicity for $x = 1$ with a thin polymer layer.

reflections are not observed in neat CholHS (see the inset of Figure 6a), a new self-assembled structure is formed upon complexation. Because the length of the CholHS molecules is ca. 2.2 nm, the polymer chains have to fold to form relatively thick layers in order to match the observed periodicity (see the scheme in Figure 8b). This is not surprising, taken the small degree of complexation, if the hydrogen bonding takes place along the P4VP chains in a random manner, i.e. noncooperatively. In the present case, the smectic structure with such a large periodicity prevails upon heating (see Figure 6b) until ca. $T_g = 71$ °C and passing the glass transition temperature the periodicity of the smectic structure decreases stepwise, obviously due to annealing effects. Upon further heating the smectic periodicity continues to decrease smoothly, until passing ca. 150 °C the distinct SAXS reflections vanish (see label "2" in Figure 6a). Instead, a broad reflection is observed due to correlation hole effects indicating the isotropic state.[52] The smectic self-assembly is recovered by cooling (see label "3" in Figure 6a). Indirectly the smooth temperature dependent SAXS also suggests that no LC-to-LC phase transitions are observed. The complex P4VP$_{5.4k}$(CholHS)$_{0.5}$ behaves qualitatively similarly, but in this case the isotropic state is achieved only by passing ca. 210 °C (see Figure 7).

Figure 8a extends the SAXS patterns to higher values of x. We use P4VP$_{5.4k}$(CholHS)$_x$ as an example, but the behavior is essentially similar for P4VP$_{50k}$(CholHS)$_x$. For $x = 0.25$ SAXS shows two equally spaced reflections (see also Figure 6), agreeing smectic order with the periodicity of 5.45 nm. Three equally spaced reflections are observed for $x = 0.50$ and $x = 0.75$ suggesting even more highly developed smectic order, and the periodicity is reduced to 5.37 and 5.35 nm, respectively. Such a behavior with thicker polymer layers for lower degrees of complexation can be explained based on statistical complexation of the hydrogen bonding side chains to the backbone instead cooperative complexation, see schematics in Figure 8b. In this way the smectic P4VP-(CholHS)$_x$ complexes behave qualitatively similarly as the hydrogen bonded P4VP-pentadecyl complexes undergoing lamellar self-assemblies without a mesogenic moiety.[13]

Regarding the nominally stoichiometric complexes P4VP-(CholHS)$_{1.0}$, characteristic SmA liquid crystallinity was already shown (Figure 3) at high temperatures near T_{ISO}, typically at $T >$ ca. 140 °C where the fluidity is sufficient. At lower temperatures, however, P4VP(CholHS)$_{1.0}$ can have complicated history-dependent structures due to competition of the LC behavior and crystalline packing of CholHS due to the high loading of dynamically hydrogen-bonded CholHS. DSC shows for P4VP(CholHS)$_{1.0}$ that near ca. 80−120 °C there exists an endotherm in heating and exotherm in cooling (Figure 4). Similar observation is made also for other highly loaded complexes with $x = 0.75$ and occasionally also for 0.5, where the latter is a limiting case (Figures S2 and S3). In analogy with previously studied comb-shaped polymeric liquid crystals with well-plasticized backbones,[34,41,53,54] we suggest that these transitions correspond to side-chain crystallization. In fact, Figure 8a shows a distinct first order reflection in addition to the equidistant second and third order reflections, corresponding to periodicity 5.32 nm (Figure 8b), which fits smoothly with the long periods of the smectic orders of P4VP$_{5.4k}$(CholHS)$_x$ with $x < 1.0$. The reflections at a larger $q > 0.2$ Å^{-1}, i.e. smaller length scale, match with those observed in neat CholHS (see Figure 8a). However, the low angle reflections of P4VP$_{5.4k}$(CholHS)$_{1.0}$ near $q = 0.1-0.15$ Å^{-1} are different from those of the pristine CholHS which suggests that in P4VP$_{5.4k}$(CholHS)$_{1.0}$ side-chain crystallization can take place sooner than crystallization as a separate phase. We also point out, that extensive annealing at elevated temperatures can also lead to a macrocopic phase separation where CholHS crystallizes out of the complex. Therefore, the structures of the near stoichiometric complexes turn to be history dependent, and in this respect more well-defined liquid crystallinity is observed for lower x.

Qualitatively, the behavior of P4VP(CholHS)$_x$ can be summarized as following. For small loading of CholHS

Table 2. Observed Morphologies of the Block Copolymer Samples with Data Acquired from SAXS and TEM[a]

			structure size (nm)	
	x	structure	polymer-complex length scale: between P4VP and CholHS (SAXS)	block copolymer length scale: between P4VP(CholHS)$_x$ and PS (TEM)
PS$_{40k}$-*b*-P4VP$_{5.6k}$(CholHS)$_x$	0	SPH		16
	0.25	sm-*in*-CYL	4.0	30
	0.50	sm-*in*-CYL	5.2	27
	0.75	sm-*in*-LAM	5.2/5.1[b]	36
	1.0	sm-*in*-LAM	5.2	28
PS$_{252k}$-*b*-P4VP$_{43k}$(CholHS)$_x$	0	SPH		35
	1.0	sm-*in*-LAM	6.1[b]	115
PS$_{422k}$-*b*-P4VP$_{63k}$(CholHS)$_x$	0	SPH		32
	1.0	sm-*in*-LAM	4.5/4.8[b]	120

[a] SPH = spherical, CYL = cylindrical, and LAM = lamellar; block copolymer structure shown in capitals, the P4VP(CholHS)$_x$ smectic structure in small letters. For cylindrical structures, the distance between two cylinders indicated; For spherical structures, the average diameter of the spheres is indicated, due to relatively large distribution in distance. [b] Size resolved from TEM.

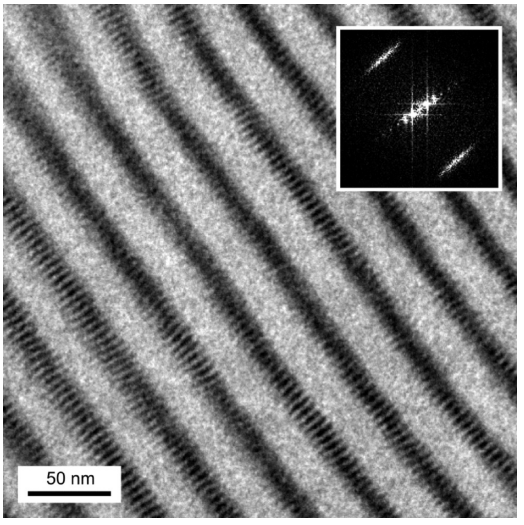

Figure 9. PS$_{40k}$-*b*-P4VP$_{5.6k}$(CholHS)$_{0.75}$: An example TEM image of a smectic-*within*-lamellar hierarchical structure. Sample is stained with iodine, which selectively stains the P4VP chains, thus both PS and CholHS show up as lighter regions. Inset shows fast Fourier transformation of the image, indicating that the hierarchical structures are perpendicular to each other.

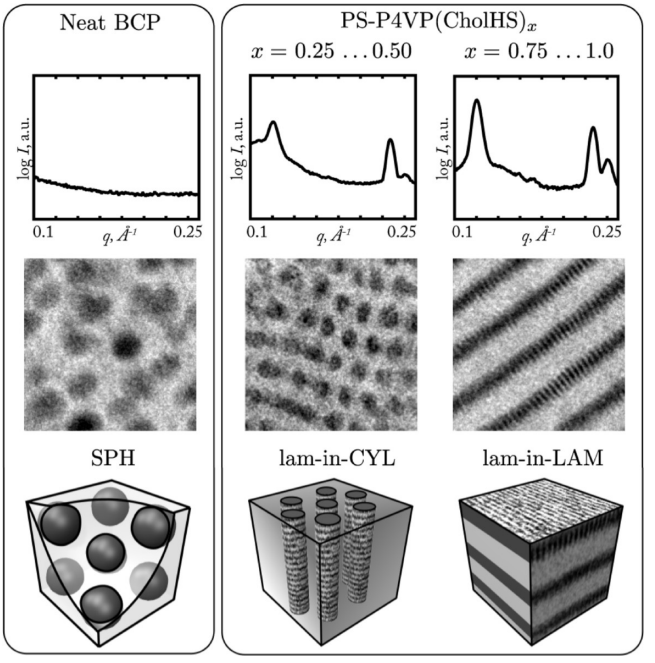

Figure 10. SAXS curves show that there is ordering of the mesogens in PS-P4VP(CholHS)$_x$ complexes and TEM images show the observed larger morphologies. For sm-*in*-LAM also the inner structure can be seen in TEM. For sm-*in*-CYL the small structure is seen in the SAXS pattern showing two orders of peaks along with peaks corresponding to side-chain crystallization. For the neat PS-*b*-P4VP no small structure exists, and TEM shows a spherical morphology.

(x = 0.25, 0.50) the complex forms a SmA mesophase and at high temperatures isotropization is observed. The experiments indicated reversibility, stability, and no crystallization phenomena were observed at the time scale of the measurements. For high loading (x = 0.75, 1.0) of P4VP(CholHS)$_x$, SmA liquid crystalline behavior was observed even in this case, while side chain crystallization and crystallization can compete depending on the thermal history. We therefore tentatively suggest that the liquid crystalline phases may be metastable toward side-chain crystallization, especially at high loading of CholHS.

Previously CholHS has been complexed with poly(dimethylamino ethyl methacrylate) and liquid crystallinity was observed.[35] Therein proton transfer was suggested between the polymer and the carboxylic acid group of CholHS and the resulting complex forms a smectic mesophase with a period of 5.48 nm confirmed by SAXS. They also conclude that 2−3% of the mesogens are crystallized in the complex, which supports our observations of side-chain crystallization. In the case of our study, the interaction is clearly hydrogen bonding. Also, hyperbranched pyridine-functionalized polyglycerol hydrogen-bonded with CholHS shows SmA phases along with crystallinity at low temperatures.[37]

Hierarchical Self-Assembly in PS-*b*-P4VP(CholHS)$_x$. Previously the supramolecular combination of block copolymer and hydrogen-bonded surfactants have been very useful to demonstrate two level hierarchical self-assembly, nonconventional phase behavior, and temperature-driven switching of electrical conductivity and photonic bandgap.[3,18,43,55] Encouraged by these observations we next studied block copolymers of polystyrene-*block*-poly(4-vinylpyridine) (PS-*b*-P4VP) with various block lengths and hydrogen-bonded CholHS. The block copolymers and the complexes are summarized in Table 2. The structures were identified using SAXS and TEM. All used neat block copolymers have a relatively short P4VP chain, thus leading to spherical self-assembly with P4VP spheres in PS matrix without the complexation.

As an illustrative example, PS-*b*-P4VP is selected with the block lengths of PS and P4VP of 40 000 g/mol and 5600 g/mol, respectively. The nominal degree of complexation

Table 3. T_g and T_{ISO} based on DSC, 10 °C/min

	T_g[PS]/T_{ISO} (°C)				
	x = 0.00	x = 0.25	x = 0.50	x = 0.75	x = 1.00
PS_{40k}-*b*-$P4VP_{5.6k}$(CholHS)$_x$	106/-	99/-	97/115	98/162	98/172

x = 0.75 is incorporated, to form the complex PS_{40k}-*b*-$P4VP_{5.6k}$(CholHS)$_{0.75}$. Figure 9 shows a TEM image of the structural hierarchy of a block copolymer/mesogen complex by showing the microphase-separated PS layers (light gray) and P4VP(CholHS) (darker) with a periodicity of 36 nm. Within the latter domains there is another level of smectic self-assembly between the P4VP and CholHS with a periodicity of 5.1 nm which agrees well with the periodicities observed in the homopolymeric P4VP(CholHS) smectic self-assemblies. The two structures seem perpendicular to each others (see fast Fourier transformation analysis in inset of Figure 9). The self-assembly is hierarchical and will be denoted as smectic-*within*-lamellar. The weight fraction of the P4VP domains can be effectively tuned by the weight fractions of the hydrogen-bonded CholHS within the P4VP domains. For example, taken first neat PS_{40k}-*b*-$P4VP_{5.6k}$, the structure consists of P4VP spheres in the PS matrix (x = 0), as expected for a block copolymer with a minority block weight fraction of only 12.3%. For the nominal degrees of complexation x = 0.25 and 0.50, the effective weight fraction increases and P4VP(CholHS) cylinders are observed within the PS matrix. In SAXS, we can observe a short period corresponding to P4VP(CholHS) smectic lamellae (see Figure 10), and we denote the structure as smectic-*within*-cylindrical. For x = 0.25, only the first order peak was observed. However patterns observed in POM give further confirmation that the inner structure is smectic. Finally, for x = 0.75 and 1.0 smectic-*within*-lamellar order is observed in TEM, in analogy with Figure 9.

Finally, we preliminarily investigated the thermal behavior of the block copolymer complex using PS_{40k}-*b*-$P4VP_{5.6k}$(CholHS)$_x$ by DSC. Results are summarized in Table 3. Therein, the glass transitions of P4VP within the neat PS_{40k}-*b*-$P4VP_{5.6k}$ could not be resolved, obviously due to its small weight fraction and as it overlaps with T_g of PS. Even in the complexes the T_g could not be reliably determined. Interestingly, CholHS was also observed to modify the transitions of the PS phase in repeated thermal cycling, which leads to reduction of T_g of PS from 106 °C to about 98 °C. This indicates that CholHS is not confined solely in the P4VP domains, but there exists an equilibrium where a small amount of CholHS leaves the P4VP domains and migrates also to the PS domains during the heating process. In a related system consisting of pentadecylphenol (PDP) added to PS-*b*-P4VP to construct self-assemblies of the P4VP(PDP) phases, it was observed that minor amounts of PDP migrate also into PS during heating.[43] Because the glass transition temperature does not drop as a function of added CholHS, it is suggested that the amount of CholHS in PS does not change.

Conclusion

A series of hydrogen-bonded complexes of poly(4-vinylpyridine) and cholesteryl hemisuccinate, P4VP(CholHS)$_x$ were prepared and their thermal transitions, morphology, and birefringence were studied using two molecular weights of P4VP. In all studied complexes, with x = 0.25, 0.50, 0.75, and 1.00, the system self-assembled into a smectic A structure with a long period of 5.3−5.9 nm, as confirmed by SAXS, TEM, and POM. The CholHS molecules are aligned end-to-end and they form a double layer between the polymer chains, and the polymer layer adopts a more coiled conformation as the degree of complexation is reduced. As observed in DSC and POM, the system turns isotropic at 130−210 °C depending on the degree of complexation. Cooling from the isotropic melt, birefringent patterns are seen in POM. The patterns quickly disappear when the smectic A mesophase of the material switches form homogenously aligned to homeotropically aligned, as the mesogens can be aligned perpendicular to the substrate by pressing the coverslip. Approaching the nominally full complexation x = 1.0, competing crystallization manifests, in particular if the samples have experienced prolonged stay at elevated temperatures. Finally hierarchical self-assemblies were constructed by combining block copolymer PS-*b*-P4VP and CholHS where TEM was used to resolve the structure in detail. We expect the shown complexes could lead toward responsive materials and self-assemblies, also taken the chirality of CholHS.

Acknowledgment. Academy of Finland and the Finnish Funding Agency for Technology and Innovation (TEKES) are gratefully acknowledged for funding. Agnieszka Iwan and Janne Ruokolainen are thanked for numerous discussions. O.I. expresses thanks for hospitality during the stay at CEA-Grenoble. Susanna Junnila is thanked for discussions and help interpreting the data. This work made use of Helsinki University of Technology, Nanomicroscopy Center (TKK-NMC) Facilities, as supported in part by the Center of New Materials.

Supporting Information Available: Figures showing full FT-IR spectra for P4VP/CholHS complexes and DSC thermograms of P4VP(CholHS) complexes. This material is available free of charge via the Internet at http://pubs.acs.org.

References and Notes

(1) Whitesides, G. M.; Mathias, J. P.; Seto, C. T. *Science* **1991**, *254*, 1312–1319.
(2) Muthukumar, M.; Ober, C. K.; Thomas, E. L. *Science* **1997**, *277*, 1225–1232.
(3) Ruokolainen, J.; Mäkinen, R.; Torkkeli, M.; Mäkelä, T.; Serimaa, R.; ten Brinke, G.; Ikkala, O. *Science* **1998**, *280*, 557–560.
(4) Whitesides, G. M.; Grzybowski, B. *Science* **2002**, *295*, 2418–2421.
(5) Ikkala, O.; ten Brinke, G. *Science* **2002**, *295*, 2407–2409.
(6) Kato, T. *Science* **2002**, *295*, 2414–2418.
(7) Faul, C. F. J.; Antonietti, M. *Adv. Mater.* **2003**, *15*, 673–683.
(8) Park, J.-W.; Thomas, E. L. *Adv. Mater.* **2003**, *15*, 585–588.
(9) Hamley, I. W. *Angew. Chem., Int. Ed.* **2003**, *42*, 1692–1712.
(10) Hammond, M. R.; Mezzenga, R. *Soft Matter* **2008**, *4*, 952–961.
(11) Antonietti, M.; Conrad, J.; Thünemann, A. *Macromolecules* **1994**, *27*, 6007–6011.
(12) Zheng, W.-Y.; Wang, R.-H.; Levon, K.; Rong, Z. Y.; Taka, T.; Pan, W. *Macromol. Chem. Phys.* **1995**, *196*, 2443–2462.
(13) Ruokolainen, J.; ten Brinke, G.; Ikkala, O.; Torkkeli, M.; Serimaa, R. *Macromolecules* **1996**, *29*, 3409–3415.
(14) Dufour, B.; Rannou, P.; Fedorko, P.; Djurado, D.; Travers, J. P.; Pron, A. *Chem. Mater.* **2001**, *13*, 4032–4440.
(15) Thünemann, A. F. *Prog. Polym. Sci.* **2002**, *27*, 1473–1572.
(16) Dufour, B.; Rannou, P.; Djurado, D.; Janeczek, H.; Zagorska, M.; de Geyer, A.; Travers, J.-P.; Pron, A. *Chem. Mater.* **2003**, *15*, 1587–1592.
(17) Kosonen, H.; Valkama, S.; Ruokolainen, J.; Torkkeli, M.; Serimaa, R.; ten Brinke, G.; Ikkala, O. *Eur. Phys. J.* **2003**, *10*, 69–75.
(18) Valkama, S.; Kosonen, H.; Ruokolainen, J.; Torkkeli, M.; Serimaa, R.; ten Brinke, G.; Ikkala, O. *Nat. Mater.* **2004**, *3*, 872–876.
(19) Ikkala, O.; ten Brinke, G. *Chem. Commun.* **2004**, 2131–2137.
(20) Ponomarenko, E. A.; Tirrell, D. A.; MacKnight, W. J. *Macromolecules* **1996**, *29*, 8751–8758.
(21) Ponomarenko, E. A.; Tirrell, D. A.; MacKnight, W. J. *Macromolecules* **1998**, *31*, 1584.
(22) Hanski, S.; Junnila, S.; Almásy, L.; Ruokolainen, J.; Ikkala, O. *Macromolecules* **2008**, *41*, 866–872.

(23) Ramani, R.; Hanski, S.; Laiho, A.; Tuma, R.; Kilpeläinen, S.; Tuomisto, F.; Ruokolainen, J.; Ikkala, O. *Biomacromolecules* **2008**, *9*, 1390–1397.
(24) Junnila, S.; Hanski, S.; Oakley, R. J.; Nummelin, S.; Ruokolainen, J.; Faul, C. F. J.; Ikkala, O. *Biomacromolecules* **2009**, *10*, 2787–2794.
(25) Bazuin, C. G.; Tork, A. *Macromolecules* **1995**, *28*, 8877–8880.
(26) Osuji, C.; Chao, C.-Y.; Bita, I.; Ober, C. K.; Thomas, E. L. *Adv. Funct. Mater.* **2002**, *12*, 753–758.
(27) de Wit, J.; Alberda van Ekenstein, G.; Polushkin, E.; Kvashnina, K.; Bras, W.; Ikkala, O.; ten Brinke, G. *Macromolecules* **2008**, *41*, 4200–4204.
(28) Han, X.; Zhang, S.; Shanks, R. A.; Pavel, D. *React. Funct. Polym.* **2008**, *68*, 1097–1102.
(29) Priimagi, A.; Cattaneo, S.; Ras, R. A. H.; Valkama, S.; Ikkala, O.; Kauranen, M. *Chem. Mater.* **2005**, *17*, 5798–5802.
(30) Zhang, Q.; Bazuin, C. G.; Barrett, C. J. *Chem. Mater.* **2008**, *20*, 29–31.
(31) Priimagi, A.; Vapaavuori, J.; Rodriguez, F. J.; Faul, C. F. J.; Heino, M. T.; Ikkala, O.; Kauranen, M.; Kaivola, M. *Chem. Mater.* **2008**, *20*, 6358–6363.
(32) Reinitzer, F. *Monatsh. Chem.* **1888**, *9*, 421–441.
(33) Platé, N. A.; Shibaev, V. P., *Comb-Shaped Polymers and Liquid Crystals*; Plenum Press: New York and London, 1987.
(34) Yamaguchi, T.; Asada, T.; Hayashi, H.; Nakamura, N. *Macromolecules* **1989**, *22*, 1141–1144.
(35) Gohy, J.-F.; Antoun, S.; Sobry, R.; Bossche, G. V. d.; Jérôme, R. *Macromol. Chem. Phys.* **2000**, *201*, 31–41.
(36) Matsusaki, M.; Fuchida, T.; Kaneko, T.; Akashi, M. *Biomacromolecules* **2005**, *6*, 2374–2379.
(37) Felekis, T.; Tziveleka, L.; Tsiourvas, D.; Paleos, C. M. *Macromolecules* **2005**, *38*, 1705–1710.
(38) Ma, X.-J.; Shen, Y.-T.; Deng, K.; Tang, H.; Lei, S.-B.; Wang, C.; Yang, Y.-L.; Feng, X.-Z. *J. Mater. Chem.* **2007**, *17*, 4699–4704.
(39) Zhou, Y.; Kasi, R. M. *J. Polym. Sci. Polym. Chem.* **2008**, *46*, 6801–6809.
(40) Cui, Z.; Zhang, Y.; He, S. *Colloid Polym. Sci.* **2008**, *286*, 1553–1559.
(41) Ahn, S.-K.; Le, L. T. N.; Kasi, R. M. *J. Polym. Sci. Polym. Chem.* **2009**, *47*, 2690–2701.
(42) Zhou, Y.; Briand, V. A.; Sharma, N.; Ahn, S.-K.; Kasi, R. M. *Materials* **2009**, *2*, 636–660.
(43) Valkama, S.; Ruotsalainen, T.; Nykänen, A.; Laiho, A.; Kosonen, H.; ten Brinke, G.; Ikkala, O.; Ruokolainen, J. *Macromolecules* **2006**, *39*, 9327–9336.
(44) Tung, S.-H.; Kalarickal, N. C.; Mays, J. W.; Xu, T. *Macromolecules* **2008**, *41*, 6453–6462.
(45) Yashima, E.; Maeda, K.; Furusho, Y. *Acc. Chem. Res.* **2008**, *41*, 1166–1180.
(46) Florián, J.; Kubelková, L.; Kotrla, J. *J. Mol. Struct.* **1995**, *349*, 435–438.
(47) Ruokolainen, J.; Tanner, J.; ten Brinke, G.; Ikkala, O.; Torkkeli, M.; Serimaa, R. *Macromolecules* **1995**, *28*, 7779–7784.
(48) Ruokolainen, J.; Torkkeli, M.; Serimaa, R.; Vahvaselkä, S.; Saariaho, M.; ten Brinke, G.; Ikkala, O. *Macromolecules* **1996**, *29*, 6621–6628.
(49) Lee, J. Y.; Painter, P. C.; Coleman, M. M. *Macromolecules* **1988**, *21*, 954.
(50) Coleman, M. M.; Graf, J. F.; Painter, P. C. *Specific Interactions and the Miscibility of Polymer Blends*; Technomic: Lancaster, PA, 1991.
(51) Luyten, M. C.; Alberda van Ekenstein, G. O. R.; ten Brinke, G.; Ruokolainen, J.; Ikkala, O.; Torkkeli, M.; Serimaa, R. *Macromolecules* **1999**, *32*, 4404.
(52) Huh, J.; Ikkala, O.; ten Brinke, G. *Macromolecules* **1997**, *30*, 1828–1835.
(53) Komiya, Z.; Pugh, C.; Schrock, R. R. *Macromolecules* **1992**, *25*, 6586–6592.
(54) Pugh, C.; Kiste, A. L. *Prog. Polym. Sci.* **1997**, *22*, 601–691.
(55) Ruokolainen, J.; ten Brinke, G.; Ikkala, O. T. *Adv. Mater.* **1999**, *11*, 777–780.